High Power Density PCB Coil Array Applied to Domestic Induction Heating Appliances

J. Serrano[(1)], J. Acero[(1)], I. Lope[(2)], C. Carretero[(3)], J.M. Burdío[(1)].

[(1)]Department of Electronic Engineering and Communications. Universidad de Zaragoza.
Maria de Luna, 1. 50018 Zaragoza. Spain.
[(2)]B/S/H/ Home Appliances Group.
Avda. de la Industria, 49. 50016 Zaragoza. Spain.
[(3)]Department of Applied Physics. Universidad de Zaragoza.
Pedro Cerbuna, 12. 50009 Zaragoza, Spain.
E-mail: jserrano@unizar.es

***Abstract*—Printed circuit board technology provides a cost constrained manufacturing option for low profile inductors due to its highly standardized process, however, the transferred power is limited by the losses in the winding, which may produce overheating. In this work, PCB inductors are evaluated for a high power application as domestic induction heating appliances. Moreover, in the seek of flexible cooking surfaces which can adapt to the size and shape of the pot, the use of partially overlapped inductors generating coil arrays is considered. The work includes the analysis of the coupling between overlapped coils when placed under a dissipative material, a study of the losses in the winding considering rectangular cross section conductors and presents the main implementation techniques. The method is employed for the design of a prototype which was tested under real working conditions delivering up to 4.2 kW.**

***Keywords*— Domestic induction heating, PCB coil, magnetic coupling.**

I. Introduction

A domestic induction cooktop [1, 2] makes use of an inductor to generate an alternating magnetic field in the range of tens of kilohertz, which reaches the base of the pot. As the pot is made of a conductor material, induced currents are generated which heats up the vessel due to Joule's heating. Additionally, if the material is ferromagnetic, extra losses are produced by magnetic hysteresis.

The inductor is usually a planar coil wound with litz wire, which presents low losses in the operation range. This cable provides efficiencies up to 98 % but involves a high cost in the production stage. In [3], PCB windings were proposed as a cost constrained solution, with a standardized production and high repeatability. However, PCB coils present lower efficiencies and are limited in power by the temperature that the substrate is able to stand.

Market forces are leading manufacturers to design and produce flexible cooking surfaces which are not limited to the number of vessels and are able to adapt to different pot shapes [4]. In the case of flexible cooking areas, small inductors are needed to provide the sufficient resolution to adapt to different pots. This penalizes the efficiency, as it is related to the inductor diameter [5] and therefore, cannot be assumed by PCB coils. The proposed solution to increase the diameter of the coils while preserving the flexibility is the use of partially overlapped inductors. This concept is shown in Fig. 1.

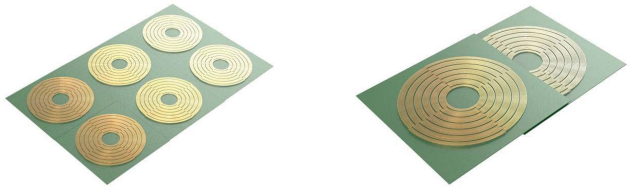

(a) (b)

Fig. 1. Flexible cooking surface. (a) Conventional approach with adjacent coils. (b) Proposed approach with overlapped coils.

The aim of this paper is to evaluate the concept of overlapped PCB coils for domestic induction heating applications. This presents a main challenge: The power levels of conventional litz inductors have to be maintained while using a much more restricted technology in terms of geometry and temperature. The necessary clearance areas between PCB tracks significantly reduces the copper fill factor. This leads to a severe reduction of the conduction cross section, which decreases in approximately 50 % from conventional litz inductors to PCB implementations. Moreover, a litz inductor is commonly 2-3 mm thick, while a PCB coil barely exceeds 0.7 mm. Therefore, PCB designs are extremely compact and need to deal with high power densities making thermal management an important issue.

The paper is organized as follows. In the first section, the model of two coupled coils in dissipative media will

978-1-5386-1180-7/18/$31.00 ©2018 IEEE

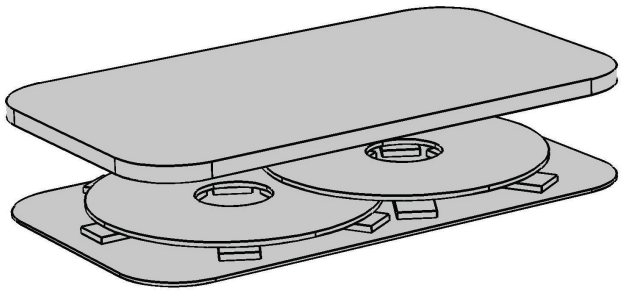

Fig. 2. Model of two coils over an aluminum shielding sheet, ferrites acting as flux concentrator and load.

Fig. 3. PCB-adapted litz structure.

be presented. In the second section, the losses in PCB windings will be analyzed. Section III presents the design and implementation of the prototype and in Section IV the experimental characterization is performed. Finally, conclusions are drawn in Section V.

II. Coupled inductors in dissipative media

A two-coil system is commonly described by its impedance matrix, **Z**, [6], which relates the currents through the coils, **I**, with the voltage drops across, **V** them as:

$$\begin{bmatrix} V_1(\omega) \\ V_2(\omega) \end{bmatrix} = \begin{bmatrix} Z_{11}(\omega) & Z_{12}(\omega) \\ Z_{21}(\omega) & Z_{22}(\omega) \end{bmatrix} \cdot \begin{bmatrix} I_1(\omega) \\ I_2(\omega) \end{bmatrix} \quad (1)$$

The elements of the impedance matrix can be obtained by means of FEM simulations on a model as the one shown in Fig. 2. The method presented in [6, 7] has been employed to obtain the values of **Z**. This method is based in setting a current in the coils and obtaining the electric field as solution, which by integration, lead to the voltage drop in each coil. Two simulations are needed. Firstly, coil 1 is activated by setting a current $I_1 = 1$ A, and I_2 is turned off ($I_2 = 1$ A). The generated voltages V_1 and V_2 are obtained. This scenario leads to $V_1 = Z_{11} \cdot I_1$ and $V_2 = Z_{21} \cdot I_2$ from where the elements Z_{11} and Z_{21} are calculated. Analogously, the elements Z_{22} and Z_{12} can be obtained by simulating when $I_1 = 0$ A, and $I_2 = 1$ A.

III. Losses in PCB windings

In order to minimize the losses in the winding, PCB-adapted litz structure has been used [8]. This structure applies a transposition pattern to the conductive tracks. Two-layer PCBs are needed so that tracks are displaced and moved to another layer generating a rotation pattern. With this method the strands become equivalent, driving the same current and reducing bundle effects [9–12]. The PCB-adapted litz structure

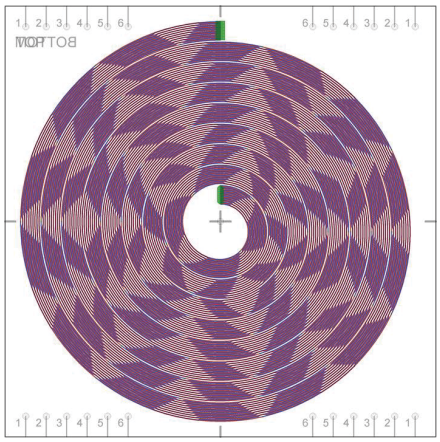

(a)

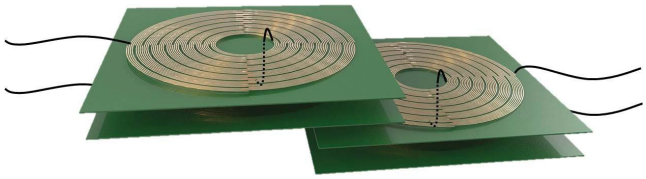

(b)

Fig. 4. Implementation of the PCB inductors. (a) PCB layout. (b) Schematic arrangement and connecitions.

is shown schematically in Fig. 3. Models for calculating the losses are available in literature [13], providing the following expressions for the winding loss resistance, R_w.

$$R_w = \underbrace{\frac{n_t}{n_s}\frac{MLT}{\sigma wh}}_{dc\ losses} \underbrace{\Phi_{\text{skin}}\left(\frac{wh}{\delta^2}, \frac{w}{h}\right)}_{skin\ losses} + \ldots \underbrace{n_t^3 n_s \frac{4\pi}{\sigma}\Phi_{\text{prox}}\left(\frac{wh}{\delta^2}, \frac{w}{h}\right)\left\langle \bar{H}_t^2 \right\rangle}_{proximity\ effects} \quad (2)$$

where n_t is the number of turns, n_s is the number of strands, MLT is the mean length turn, σ in the electrical conductivity, w is the track width, h is the track height, δ is the skin depth, $\left\langle \bar{H}_t^2 \right\rangle$ is the average squared magnetic field in the coil per current unit, and Φ_{skin} and Φ_{prox} are functions including geometry and frequency dependences, which can be approximated by 1 and $\frac{w}{12\pi h}\left(\frac{wh}{\delta^2}\right)^2$ respectively if $\frac{wh}{\delta^2} \leq 1$.

IV. Inductor design and implementation techniques

The inductor was designed with 16 turns of 21 strands. The tracks were dimensioned to minimize the loss resistance according to equation 2, which gave as result a track width of $\omega = 500$ µm and copper thickness of $h = 210$ µm. Due to the geometric restrictions in PCBs, two boards were needed

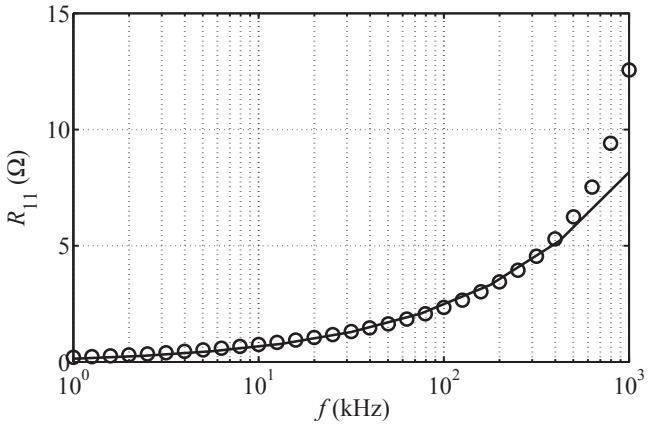

(a)

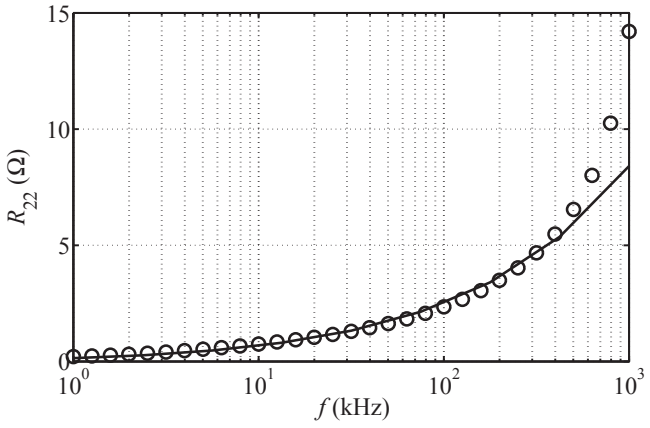

(b)

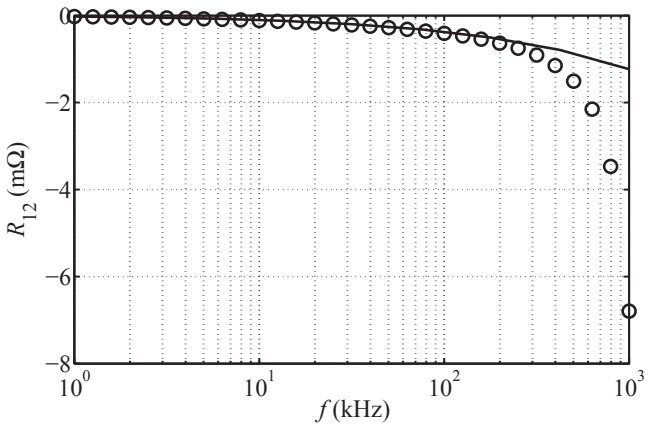

(c)

Fig. 5. Resistance matrix of a double-inductor system with a ferromagnetic load. Simulation in solid line, measurements in circles. (a) Self-resistance of coil 1. (b) Self-resistance of coil 2. (c) Coupling term.

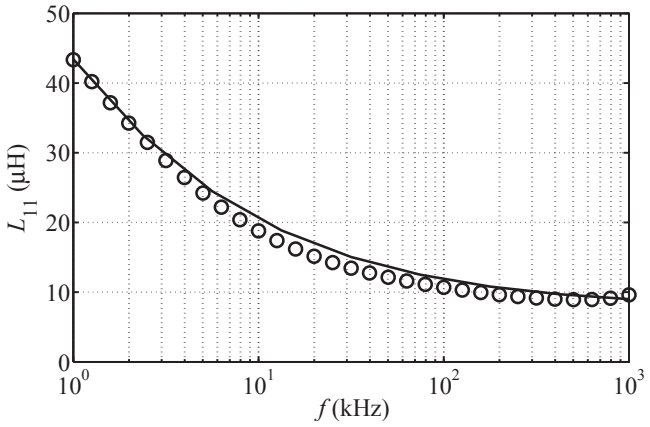

(a)

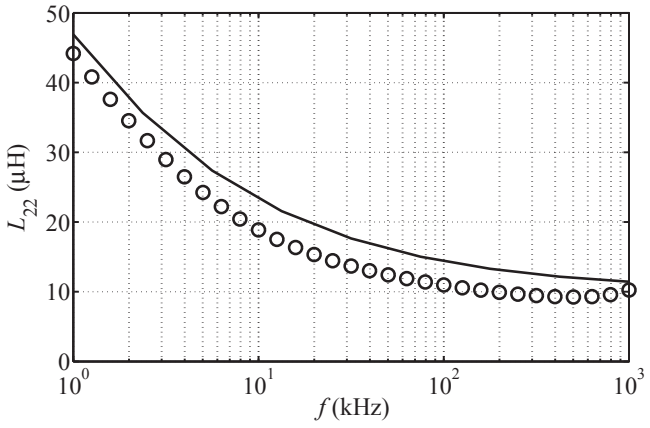

(b)

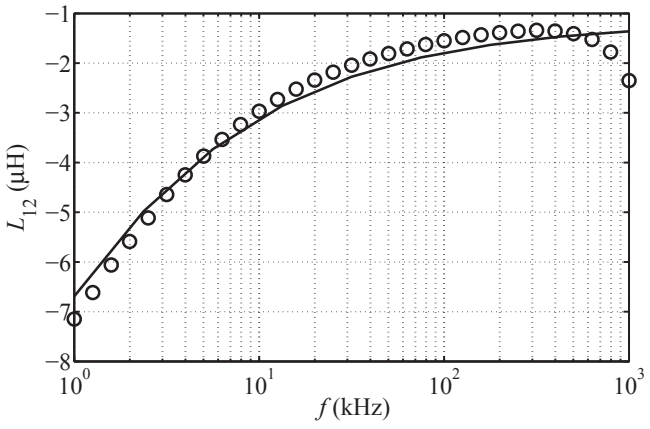

(c)

Fig. 6. Inductance matrix of a double-inductor system with a ferromagnetic load. Simulation in solid line, measurements in circles.(a) Self-inductance of coil 1. (b) Self-inductance of coil 2. (c) Coupling term.

for each inductor, which were stacked and connected in series. The PCB layout and the stacking method are shown in Fig. 4. Note that, in each PCB stack, one of the board has to be flipped so that the magnetic fields generated by each of the boards are added and not canceled.

In order to keep the coils as close as possible to the vessel, the PCBs have been manufactured on a 200 μm substrate. Moreover, the series connection between PCBs has been done by soldering a pad on one of the boards to a pad on the other

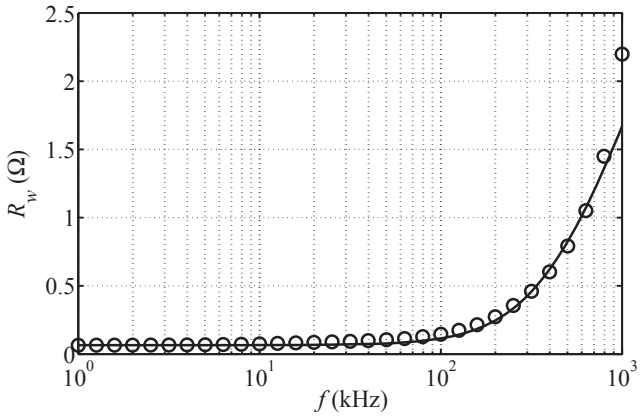

Fig. 7. Winding resistance. Simulation in solid line, measurements in circles.

board. This optimizes space and leads to an extremely thin stack (under 600 μm) compared to litz-wire inductors, which are usually 2 mm to 3 mm thick. The selected substrate is a high thermal performance FR-4 with glass transition at $T_g = 180$ °C.

V. Experimental validation

A. Small signal characterization

The coils were measured making use of an Agilent E4980A LCR Meter with a ferromagnetic load covering both coils. While self-impedances, Z_{11} and Z_{22} can be measured directly at the coils terminals, the coupling impedances are obtained by measuring the series connection of both coils, Z_s, and the counter-series connection, Z_{cs} [7]:

$$Z_{12} = Z_{21} = \frac{Z_s - Z_{cs}}{4}. \tag{3}$$

The elements of the impedance matrix are commonly represented as a resistance in series with an inductance, and therefore, each impedance can be expressed as $Z_{ij} = R_{ij} + j\omega L_{ij}$. Fig. 5 compares the measurements with the simulation results for the resistive components. The inductive components are shown in Fig. 6.

Moreover, in order to verify the loss calculation, one of the inductors was measured without a load. In this scenario, there is no resistive contribution of the dissipative material, and the measured resistance corresponds to the winding ac resistance as seen in equation (2). The measured resistance of the unloaded winding is shown in Fig. 7 and compared to the calculation.

B. Large signal characterization

The arrangement was tested under real working conditions powered by a double half-bride resonant inverter. The schematic of the experimental setup is shown in Fig. 8, where

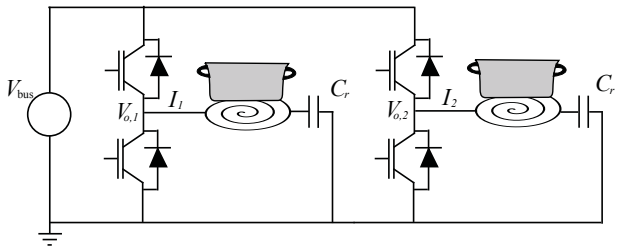

Fig. 8. Schematic of the experimental setup: Double half-bridge inverter with resonant load.

Fig. 9. Picture of the induction load composed of two partially overlapped PCB inductors and a ferromagnetic pot.

the dc bus is $V_{\text{bus}} = 230$ V and the resonant capacitor is $C_r = 700$ μF. Fig. 9 shows a picture of the induction load composed of the partially overlapped PCB inductors and a ferromagnetic pot.

The main waveforms were captured by means of a Tektronix DPO 7354 Oscilloscope with Pearson Model-110 current monitors and Tektronix P5205 differential probes. Fig.10 shows the half-bridge output voltage and the current through each of the inductors when both coils are activated at the same time delivering a total of 4.2 kW to the load.

Due to the high power delivered and the temperature limitations of PCB substrates, the temperature was monitored by means of several thermocouples. Fig. 11 shows the temperature during a prolonged test delivering 4.2 kW. The experiment shows how the temperature never reaches the glass transition temperature of the substrate, which for the chosen high temperature FR-4 is 180º

VI. Conclusions

In this work, PCB inductors have been used to conform a flexible cooking surface, which is able to deliver up to 4.2 kW. The PCB arrangement has been implemented using a high temperature ultra-thin substrate, which generates a coil with

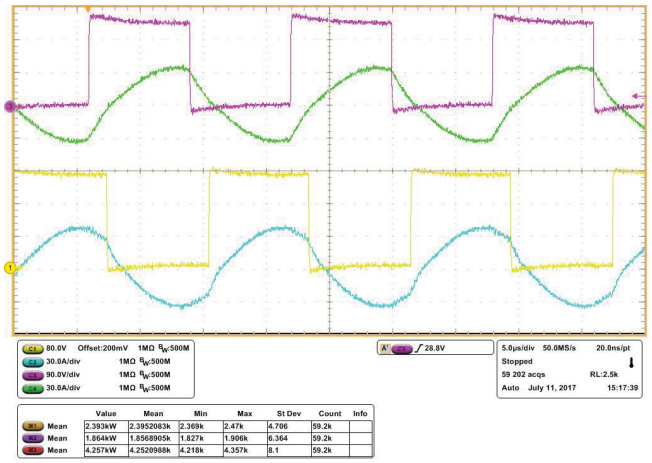

Fig. 10. Main waveforms in the converter when delivering 4.2 kW at 62.5 kHz. Output voltages $V_{o,1}$ and $V_{o,2}$ in magenta and yellow respectively (90 V/div). Currents through the inductors I_1 and I_2 in green and blue (30 A/div).

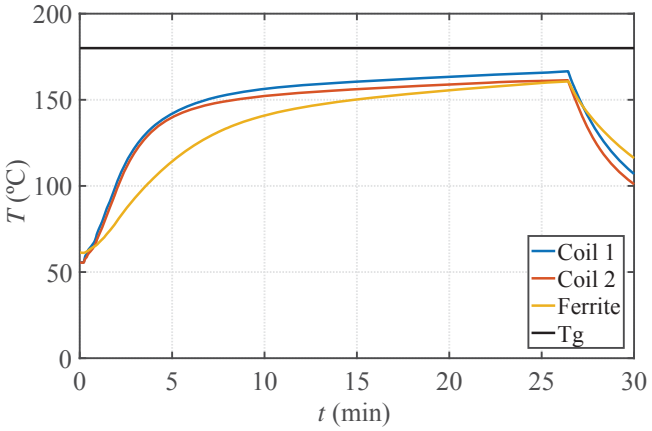

Fig. 11. Measured temperature during a prolonged test delivering 4.2 kW.

the quarter of the volume of a conventional litz-wire coil while delivering the same power. The experimental characterization is in good accordance with the simulations and the system was capable of withstanding prolonged tests at high power within the operation temperature range of the PCB substrate.

VII. Acknowledgements

This work was partly supported by the Spanish MINECO under Project TEC2016-78358-R, and Project RTC-2014-1847-6, by the Torres Quevedo Grant PTQ-14-06713, by the DGA-FSE, by the University of Zaragoza under Project JIUZ-2016-CIE-01, and by the BSH Home Appliances Group.

References

[1] F. Forest, S. Faucher, J.-Y. Gaspard, D. Montloup, J.-J. Huselstein, and C. Joubert, "Frequency-synchronized resonant converters for the supply of multiwinding coils in induction cooking appliances," *Industrial Electronics, IEEE Transactions on*, vol. 54, pp. 441–452, Feb 2007.

[2] F. Forest, E. Labouré, F. Costa, and J. Gaspard, "Principle of a multi-load/single converter system for low power induction heating," *Power Electronics, IEEE Transactions on*, vol. 15, pp. 223–230, Mar 2000.

[3] I. Lope, J. Acero, J. Burdio, C. Carretero, and R. Alonso, "Design and implementation of PCB inductors with litz-wire structure for conventional-size large-signal domestic induction heating applications," *Industry Applications, IEEE Transactions on*, vol. 51, pp. 2434–2442, May 2015.

[4] O. Lucía, J. Acero, C. Carretero, and J. Burdío, "Induction heating appliances: Toward more flexible cooking surfaces," *Industrial Electronics Magazine, IEEE*, vol. 7, pp. 35–47, Sept 2013.

[5] J. Acero, C. Carretero, R. Alonso, and J. M. Burdio, "Quantitative evaluation of induction efficiency in domestic induction heating applications," *IEEE Transactions on Magnetics*, vol. 49, pp. 1382–1389, April 2013.

[6] K. R. Davey and D. Zheng, "Prediction and use of impedance matrices for eddy-current problems," *IEEE Transactions on Magnetics*, vol. 33, pp. 2478–2485, Jul 1997.

[7] C. Carretero, O. Lucia, J. Acero, and J. M. Burdio, "Computational modeling of two partly coupled coils supplied by a double half-bridge resonant inverter for induction heating appliances," *IEEE Transactions on Industrial Electronics*, vol. 60, pp. 3092–3105, Aug 2013.

[8] I. Lope, C. Carretero, J. Acero, R. Alonso, and J. Burdío, "Frequency-dependent resistance of planar coils in printed circuit board with litz structure," *Magnetics, IEEE Transactions on*, vol. 50, pp. 1–9, Dec 2014.

[9] J. A. Ferreira and J. D. van Wyk, "A new method for the more accurate determination of conductor losses in power electronic converter magnetic components," in *Third International Conference on Power Electronics and Variable-Speed Drives*, pp. 184–187, Jul 1988.

[10] C. Sullivan and R. Zhang, "Analytical model for effects of twisting on litz-wire losses," in *Control and Modeling for Power Electronics (COMPEL), 2014 IEEE 15th Workshop on*, pp. 1–10, June 2014.

[11] X. Nan and C. R. Sullivan, "An equivalent complex permeability model for litz-wire windings," *IEEE Transactions on Industry Applications*, vol. 45, pp. 854–860, March 2009.

[12] S. Wang, M. de Rooij, W. Odendaal, J. van Wyk, and D. Boroyevich, "Reduction of high-frequency conduction losses using a planar litz structure," *Power Electronics, IEEE Transactions on*, vol. 20, pp. 261–267, March 2005.

[13] I. Lope, C. Carretero, J. Acero, R. Alonso, and J. Burdío, "AC power losses model for planar windings with rectangular cross-sectional conductors," *Power Electronics, IEEE Transactions on*, vol. 29, pp. 23–28, Jan 2014.